RESEARCH ARTICLE

Comparative transcriptome analysis provides insights into dwarfism in cherry tomato (*Solanum lycopersicum* var. *cerasiforme*)

Md Abdur Rahim[1,2], Hee-Jeong Jung[1], Khandker Shazia Afrin[1], Ji-Hee Lee[3], Ill-Sup Nou[1]*

1 Department of Horticulture, Sunchon National University, Suncheon, Republic of Korea, **2** Department of Genetics and Plant Breeding, Sher-e-Bangla Agricultural University, Dhaka, Bangladesh, **3** Center for Horticulture Seed Development of Golden Seed Project, Sunchon National University, Suncheon, Republic of Korea

* nis@sunchon.ac.kr

Abstract

Tomato, which can be eaten as a vegetable or fruit, is one of the most popular and nutritionally important crops around the world. Although most plants of the cherry tomato cultivar 'Minichal' have a normal phenotype, some plants have a stunted phenotype with reduced plant height, leaf size, and fruit size, as well as altered leaf and fruit shape. To investigate the molecular mechanisms underlying these differences, we generated RNA-seq libraries from pooled leaf samples of 10 normal (N) and 10 stunted (S) plants. Using the Illumina sequencing platform, we obtained a total of 115.45 million high-quality clean reads assembled into 35,216 genes and 35,216 transcripts. A total of 661 genes were differentially expressed between N and S plants. Of these, 420 differentially expressed genes (DEGs) were up-regulated, and 221 DEGs were down-regulated. The RNA-seq data were validated using quantitative reverse-transcription PCR. Enrichment analysis of DEGs using the Kyoto Encyclopedia of Genes and Genomes (KEGG) showed that the enriched pathways were involved in steroid biosynthesis, homologous recombination, and mismatch repair. Among these, three genes related to steroid biosynthesis, including *3BETAHSD/D2*, *DIM* and *DWF5* were down-regulated in S compared to N. Of these, *DIM* and *DWF5* are known to be involved in brassinosteroid biosynthesis. Our results thus provide a useful insight into dwarfism in cherry tomato, and offer a platform for evaluating related species.

Introduction

Cultivated tomato (*Solanum lycopersicum* L.) is nutritionally rich, economically important, and widely grown around the world. It is ranked as the second most-consumed vegetable after the potato [1]. Tomato can be consumed fresh or in processed food items such as ketchup, paste, juice, pizza sauce, and soup. The ripe tomato fruit is abundant in lycopene, a red carotenoid pigment that has antioxidant properties, which help to protect against heart diseases, and lung and prostate cancer [2–5]. It also contains other carotenoids, including beta-carotene, neurosporene, lutein, and zeaxanthin, which support the human immune system [6].

Tomato is also a good source of vitamins, minerals and bioactive phenolic compounds, including vitamin C, vitamin K, tocopherols, folate, and potassium [7].

Cherry tomato (*Solanum lycopersicum* var. *cerasiforme)* is an ancestor of the domesticated form of cultivated tomato [8]. The content of bioactive compounds is generally higher in cherry-type tomatoes than in large ones [9], and fresh cherry tomatoes contain higher levels of nutrient and phenolic compounds than their processed products [9]. Therefore, the rate of consumption of fresh tomato fruit is increasing rapidly, and cherry tomatoes, in particular, are becoming increasingly popular as a fresh salad food because of their high nutritional quality.

In this study, we characterized a stunted phenotype of the cherry tomato cultivar 'Minichal', which exhibits defective growth and development, including reduced internode length, a highly branched inflorescence and reduced fruit size compared to the normal 'Minichal' phenotype. This dwarfism ultimately reduces the economic value of this tomato cultivar.

Several previous reports have demonstrated that mutations in hormone biosynthesis and signaling genes can result in dwarfism in plants. For example, Koornneef and van der Veen [10] characterized *GA5* (*GA20ox1*) mutants in *Arabidopsis*. *GA5* is involved in gibberellic acid (GA) biosynthesis, and its mutation leads to plant dwarfism. Timpte et al. [11] described a mutation in *axr2*, which affects an auxin responsive protein and causes dwarfism in *Arabidopsis* characterized by reduced cell length and number in both hypocotyls and inflorescences, and also by reduced epidermal cell size. Notably, exogenous treatment with auxin was able to rescue the mutant phenotype [12].

In addition, several brassinolide (BL) steroids, which are collectively known as brassinosteroids (BRs) [13,14] are crucial for normal growth and development in plants [15]. BL is the most active form of BR, and is the end product of the BR biosynthesis pathway [13,16]. BRs are involved in a variety of physiological processes, including promotion of cell elongation, cell differentiation, retardation of senescence, promotion of ethylene biosynthesis, modulation of stress responses, and regulation of gene expression [17]. They are biosynthesized through two alternate pathways; the early and late C-6 oxidation pathways [15,17,18], have been studied in plant species including *Arabidopsis*, pea, rice, and tomato [18]. The enzymes catalyzing the BR biosynthesis pathway have been particularly well characterized in *Arabidopsis*, as have BR biosynthesis mutants that result in a dwarf phenotype, including *det2* [19], *dwf1* [20,21], *cpd* [22], *dwf4* [23,24], *dwf5* [25], *dwf7* [26], and *sax1* [27], and BR signaling and perception mutants [18]. Two BR biosynthesis dwarf mutants, *BR-deficient dwarf1* (*brd1*) and *ebisu dwarf* (*d2*), which exhibit stem and leaf elongation abnormalities, have been reported in rice [28]. In addition, a dwarf mutant with reduced BR levels, *lk*, has been reported in pea, and exogenous application of brassinolide restores it to a normal growth phenotype [18]. In cultivated tomato, two dwarf mutants, *dumpy* (*dpy*) and *dwarf* (*d*), have been reported, both of which are defective in BR biosynthesis [12].

Until now, little was known about the molecular mechanisms underlying dwarfism in cherry tomato. To gain insight into these molecular mechanisms, we used the Illumina sequencing platform to carry out transcriptomic analysis of leaves from normal (N) and stunted (S) tomato plants of the cultivar 'Minichal'. We identified differentially expressed genes that might be involved in dwarfism of this cherry tomato cultivar 'Minichal'. We further validated their expression pattern by qRT-PCR. These results provide a basis for identifying the key genes involved in tomato dwarfism.

Materials and methods

Plant materials

Two different phenotypes of the tomato cultivar 'Minichal', which included normal (N) plants with regular growth and development, and stunted (S) plants with reduced plant growth and

development, were used (Fig 1). These lines were grown in a glasshouse at the Department of Horticulture, Sunchon National University, Suncheon, Republic of Korea. Young leaves were sampled from 10 individual plants for each phenotypic category (N and S). Leaves were pooled and frozen in liquid nitrogen before storing them at –80˚C until required.

RNA extraction and library construction for transcriptome analysis

Total RNA was isolated from 100 mg finely powdered leaf tissues using the RNeasy Mini Kit (Qiagen, USA). The quantity and integrity were checked with a NanoDrop spectrophotometer (NanoDrop Technologies, Wilmington, Delaware, USA) and an Agilent 2100 BioAnalyzer (Agilent Technologies, Palo Alto, CA, USA). Two RNA-seq libraries were constructed by Theragen Bio Institute (Suwon, South Korea) using the TruSeq RNA Library Prep Kit (Illumina Inc.) and RNA samples with a RIN (RNA integrity number) greater than 7. RNA sequencing was performed using an Illumina HiSeq 2000 platform (Illumina Inc.). RNA sequencing data were analyzed according to the method described by Trapnell et al. [29].

Quantification of expression patterns and differentially expressed genes

Reference genome and gene model annotation files for tomato (*Solanum lycopersicum*) were retrieved from the Ensembl database (https://plants.ensembl.org/). Clean reads were mapped to the reference genome using TopHat (v.2.1.1; http://ccb.jhu.edu/). Assembled genes were searched against the Swiss-Prot database and Gene Ontology (GO) categories. Gene expression patterns and differential expression were determined using Cufflinks (v.2.0.1; http://cufflinks.cbcb.umd.edu/), as previously reported by Trapnell et al. [29]. The expression level was normalized by the number of fragments per kilobase of exon per million mapped reads (FPKM). Differentially expressed genes (DEGs) were detected using DEGseq [30] with an adjusted $p < 0.005$ and $q < 0.05$. All DEGs were subjected to GO analysis and Kyoto Encyclopedia of Genes and Genomes (KEGG) pathway enrichment analysis using WebGestalt [31] and DAVID (https://david.ncifcrf.gov/).

Validation of RNA-seq data by qRT-PCR

The expression patterns of eight genes were selected for further validation by quantitative reverse transcription PCR (qRT-PCR). cDNA was synthesized from 2 µg of high-quality total RNA using SuperScript III (Invitrogen, Gaithersburg, MD). The qRT-PCR reaction was carried out using 50 ng cDNA and a gene-specific primer (S1 Table) with 2x SyGreen Mix Lo-ROX (qPCRBIO; PCR Biosystems, London, UK) and a LightCycler 96 instrument (Roche, Mannheim, Germany). The reaction conditions were: 95˚C for 5 min, then 50 cycles at 95˚C for 10 s, 60˚C for 10 s, and 72˚C for 15 s. Cq values obtained from qRT-PCR were analyzed with LightCycler 96 software (Roche, Germany). The mean normalized expression was determined by the comparative $2^{-\Delta\Delta Ct}$ method [32], where *Elongation factor-1alpha* (*EF-1alpha*) was used as an internal control gene for *Solanum lycopersicum*.

Results

Overview of RNA sequencing

Leaves at similar stages of growth were collected and pooled from normal (N) and stunted (S) tomato plants for RNA isolation. Their transcriptomes were profiled using the Illumina sequencing platform. We obtained 117.995 million paired-end raw reads (Table 1). Subsequently, adapters, low-quality reads, and ambiguous reads were removed (Fig 2A). A final
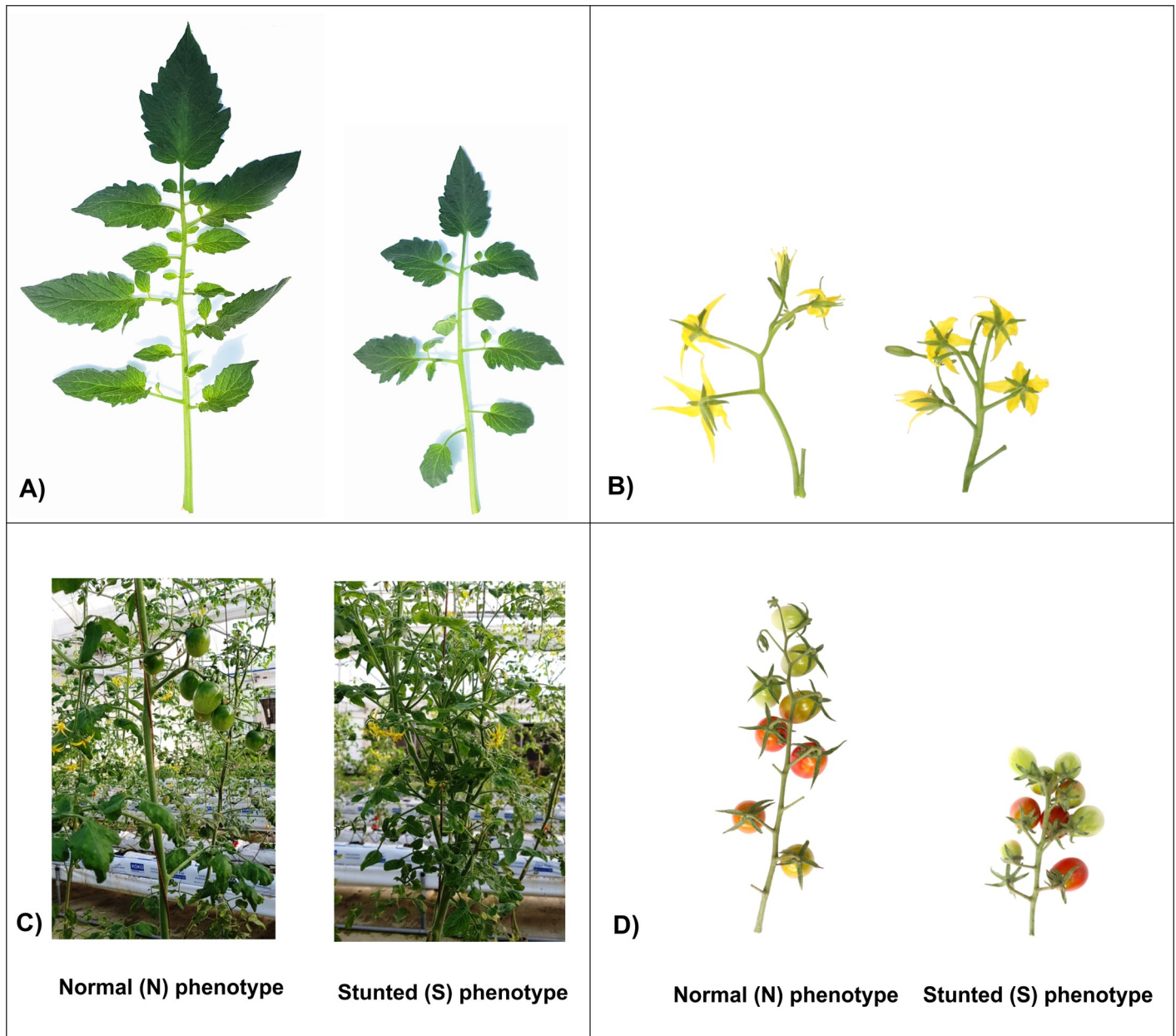
Fig 1. Phenotypes of normal (N) and stunted (S) plants of the cherry tomato cv. 'Minichal'. A) Leaves; B) inflorescences; C) fruits; D) mature plants.

total of 115.450 million high-quality clean reads were obtained (54.755 and 60.695 million for N and S, respectively) (Table 1).

A total of 97.6% reads from N plants, and 98.0% reads from S plants, were mapped to the *S. lycopersicum* reference genome (Ensembl). On average, 91.6% and 91.5% reads, respectively, uniquely mapped to the reference database. High-quality clean reads were assembled into 35,216 transcripts and 35,216 genes (Table 1). Among the annotated genes, 72% and 71% had 90–100% coverage in N and S tomato libraries, respectively (Fig 2B and 2C), indicating that the distributions of reads were similar between tomato libraries. Both the samples had Q20 scores (indicating Phred-like quality) greater than 96%, indicating the high quality of the RNA

Table 1. Overview of transcriptome sequencing and assembly to the tomato (*Solanum lycopersicum*) reference genome.

Samples	Raw reads	Clean reads n (%)	Total mapped n (%)	Uniquely mapped n (%)	READ 1/ READ 2	Strand(+)/ strand(-)	Splice reads n (%)	Q20 (%)	GC (%)
Normal (N)	56,088,460	54,754,874 (97.6)	50,766,351 (92.7)	50,139,657 (91.6)	25,334,107/ 24,805,550	24,955,309/ 25,184,348	16,552,209 (30.2)	96.60	43.47
Stunted (S)	61,907,020	60,695,416 (98.0)	56,095,234 (92.4)	55,446,956 (91.5)	28,004,215/ 27,442,741	27,602,386/ 27,844,570	18,465,751 (30.4)	96.81	43.55
Total	117,995,480	115,450,290							
Total number	Transcripts	Genes							
	35,216	35,216							

https://doi.org/10.1371/journal.pone.0208770.t001

sequencing. These high quality transcriptomic data from N and S plants therefore provide a basis for identifying the key genes involved in tomato dwarfism.

Differentially expressed genes between normal and stunted tomato pools

A total of 661 differentially expressed genes (DEGs) between N and S tomato plants were identified using the R package DEGseq (S2 Table) [30]. Of these DEGs, 420 genes were up-regulated, and 241 genes were down-regulated in S versus N (Fig 3). However, 32 DEGs were found to be expressed in S only, and 108 in N only (S2 Table). The distribution of up-regulated and down-regulated genes is shown using a volcano plot (Fig 4).

Functional classification of DEGs

Using GO analysis, DEGs were classified into three main categories: biological processes, cellular components, and molecular functions; and 50 functional groups (Fig 5). In the biological process category, 'metabolic process' (GO:0008152), 'response to stimulus' (GO:0050896), and 'biological regulation' (GO:0065007) were the most important GO terms identified; in the cellular components category, 'membrane' (GO:0016020) and 'nucleus' (GO:0005634) were most important; and in the molecular function category, 'protein binding' (GO:0005515), 'ion binding' (GO:0043167), 'nucleic acid binding' (GO:0003676), and 'hydrolase activity' (GO:0016787) were most frequently identified.

To obtain insight into the biological significance of identified DEGs, GO enrichment analysis was performed using the Gene Ontology database (http://www.geneontology.org/). Enriched GO terms for genes that were up-regulated and down-regulated between N and S tomato plants are shown in Fig 6. GO enrichment analysis revealed that 'catalytic activity' and 'metabolic process' were the most often enriched GO terms for both up-regulated and down-regulated genes (S3 Table).

Identified DEGs were also subjected to functional annotation clustering at the highest level of stringency using the DAVID database (https://david.ncifcrf.gov/). The analysis showed 22 clusters (S4 Table) with an enriched score ranging from 0.02 to 2.37. Of these, six clusters had an enrichment score greater than 1.0 (Table 2). The most enriched terms were 'steroid biosynthesis', 'WRKY transcription factor' (TF), 'DNA damage/repair', 'tetratricopeptide repeat' (TPR), 'MADS-box TF', and 'mitogen-activated protein kinases' (MAPK).

DEG pathway analysis was done using DAVID and the KEGG pathway database, using default threshold parameters except for EASY, which was set at >0.3. The results indicated that 'steroid biosynthesis', 'homologous recombination', 'mismatch repair', 'DNA replication', 'protein export', 'glucosinolate biosynthesis', 'vitamin B6 metabolism', 'nucleotide excision repair', '2-oxocarboxylic acid metabolism', 'zeatin biosynthesis', and 'cutin, suberin, and wax

A) Classification of raw reads
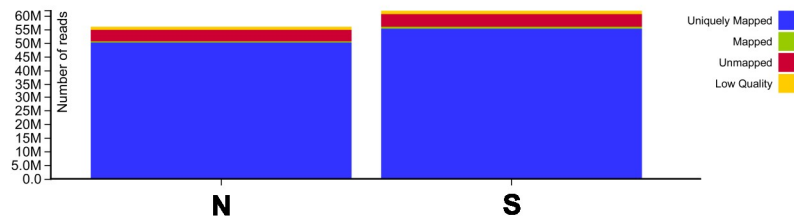
B) Distribution of genes' coverage (N)
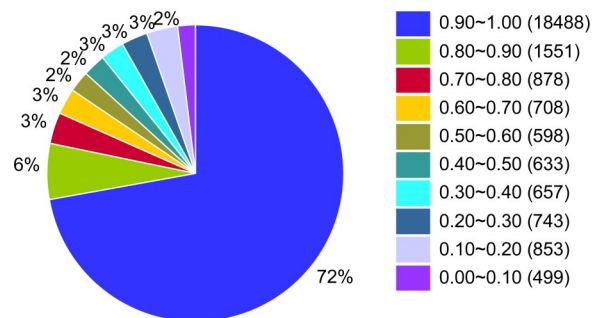
C) Distribution of genes' coverage (S)
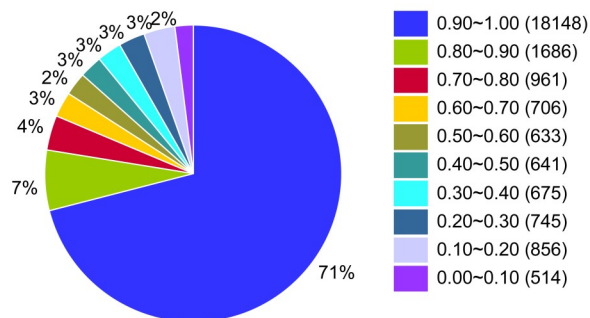
Fig 2. Quality raw reads and gene coverage of normal (N) and stunted (S) phenotypes of the cherry tomato cv. 'Minichal' using RNA-seq. A) Classification of raw reads; B) distribution of genes' coverage for normal pool (N); C) distribution of genes' coverage for stunted pool (S).

biosynthesis' were highly enriched pathways (Table 3), with the most significantly enriched pathways being 'homologous recombination' and 'steroid biosynthesis'.

Expression pattern of genes related to homologous recombination, steroid and cytokinin/zeatin biosynthesis

Transcript levels of four genes, *RPA3B* (Solyc09g009900.2), *RPA2B* (Solyc10g081830.1), XRCC3 (Solyc07g055170.1) and *RPA1E* (Solyc03g013260.1)—all related to homologous recombination—were up-regulated in stunted (S) 'Minichal' cherry tomatoes compared to

Fig 3. Number of up-regulated and down-regulated genes between normal (N) and stunted (S) cherry tomato cv. 'Minichal'.

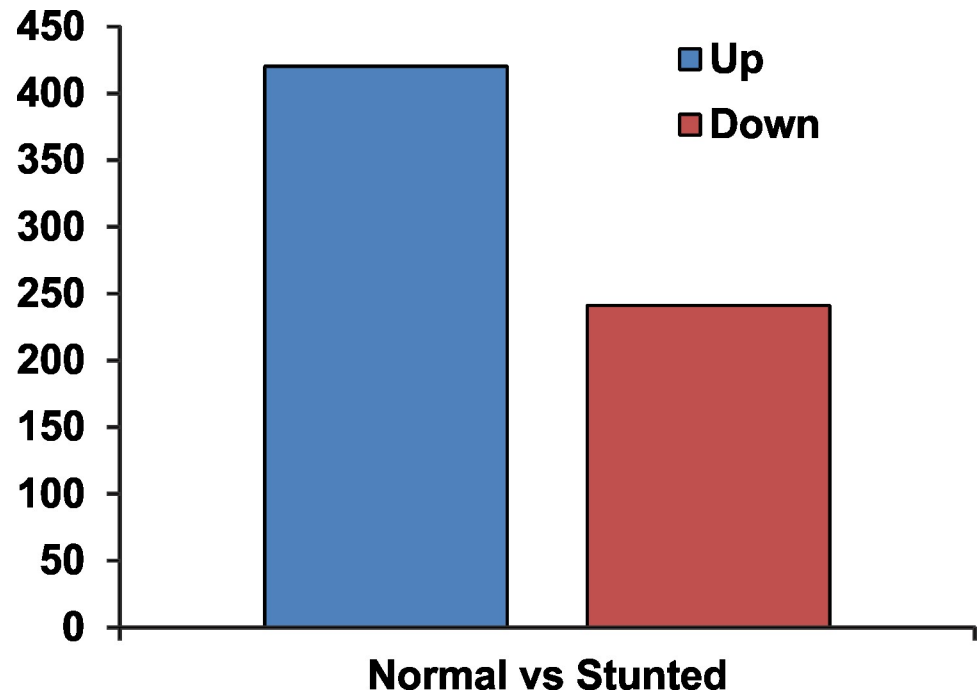those with a normal (N) phenotype. On the contrary, three genes related to the steroid biosynthetic pathway, *3BETAHSD/D2* (Solyc02g081730.2), DWF5 (Solyc06g074090.2), and DIM (Solyc02g069490.2), were down-regulated in S compared to N (Fig 7). The gene *adenylate isopentenyl transferase 3* (*IPT3*), which is involved in cytokinin biosynthesis, and *cytokinin oxidase 3* (*CKX3*), which catalyzes the degradation of cytokinins, were up-regulated in S compared to N (Fig 7), although expression of *CKX3* was higher than that of the *IPT3*.

Expression patterns of other hormone-related genes

Among the DEGs, four genes related to the auxin signaling pathway, *IAA14* (Solyc09g083290.2), *AX6B_SOYBN* (Solyc04g053010.1), *AXX15_SOYBN* (Solyc11g011650.1), and *12KD_FRAAN* (Solyc02g077880.2), were up-regulated, and two genes, *AIR12* (Solyc09g056390.1), and *AXX15_SOYBN* (Solyc04g053000.1), were down-regulated in S compared to N (Fig 8). Two ethylene biosynthetic genes, *1-aminocyclopropane-1-carboxylate oxidase 1* (*ACO1*), and *1-aminocyclopropane-1-carboxylate oxidase 3* (*ACO3*), were highly expressed in S compared to N (Fig 8). Furthermore, *ethylene responsive factor* (*ERF*) genes that lie downstream of the ethylene signaling pathway were also differentially expressed. Among these downstream genes, *ERF13* (Solyc01g090340.2) was the most highly expressed and was down-regulated in S compared to N. Expression of the remaining three *ERFs* was very low, and two of these *(ERF003*, Solyc03g117130.2, and *ERF13*, Solyc01g090310.2) were not expressed in 'N at all.

Expression patterns of WRKY TF, MADS-box TF, MAPK and TPR-related genes

The expression of four WRKY TF genes, *WRKY 40* (Solyc03g116890.2), *WRKY 41* (Solyc01g095630.2), *WRKY 50* (Solyc08g062490.2), and *WRKY 51* (Solyc12g056750.1), were
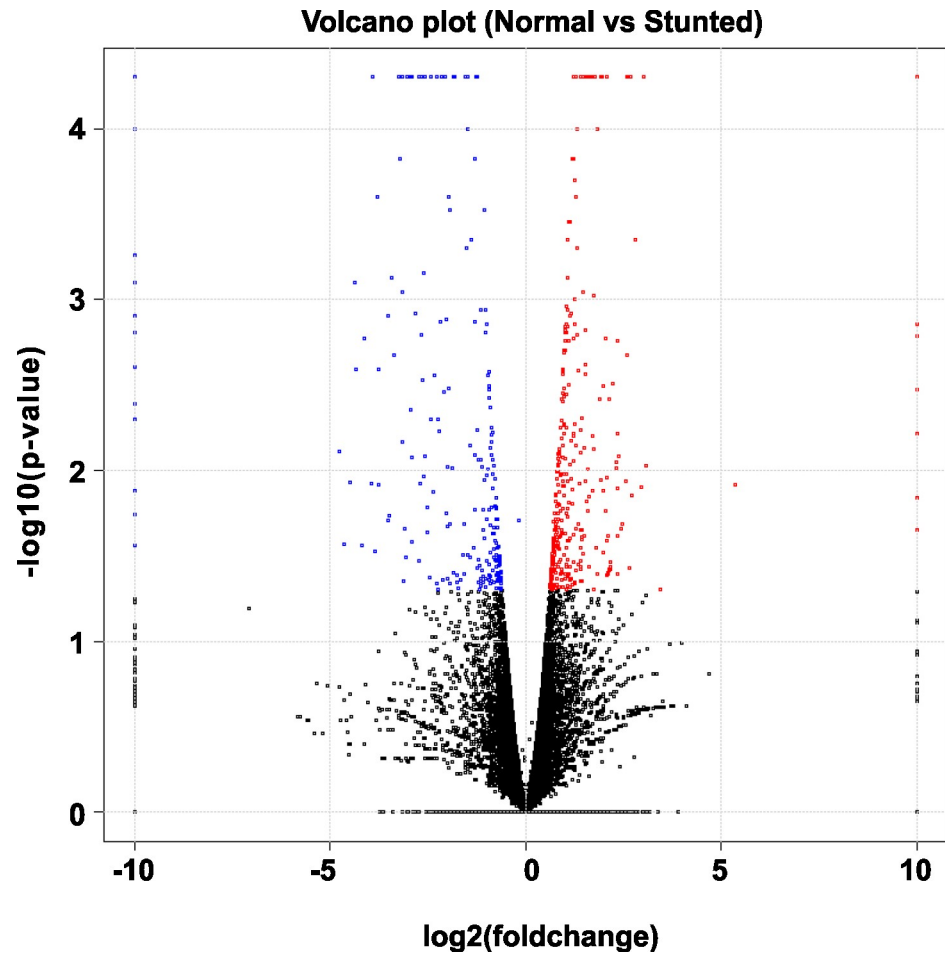
Volcano plot (Normal vs Stunted)

Fig 4. Volcano plot of differentially expressed genes (DEGs) between normal (N) and stunted (S) cherry tomato cv. 'Minichal'. X-axis and y-axis represent log2 fold-change differences between the compared samples and statistical significance as the negative log of DEG P-values, respectively. The significantly up-regulated and down-regulated genes are indicated with red and blue dots, respectively, while non-significant genes are shown as black dots.

up-regulated in S compared to N (Fig 9). Among the MADS-box TF genes, *AGL36* (Solyc01g103550.1), and *SEPALLATA 2* (Solyc02g089200.2) were up-regulated, while *SVP* (Solyc04g076280.2), and *AGL19* (Solyc08g080100.2), were down-regulated in S compared to N (Fig 9). The *YDA* (Solyc06g036080.2) gene, which encodes a mitogen-activated protein kinase (MAPK), was down-regulated in S (Fig 9). Transcript levels of three *tetratricopeptide repeat (TPR)-like* genes, *FKBP65* (Solyc10g078250.1), *LPA1* (Solyc09g063140.2), and *NOXY38* (Solyc05g050630.2), were down-regulated, while *ATSDI1* (Solyc06g007970.2) was up-regulated in S compared to N (Fig 9).

Validation of RNA-seq data

To test the reliability of RNA-seq results, qRT-PCR was used to measure the expression of eight genes with the same RNA samples used for RNA-seq. Relative expression of the tested genes was consistent with the RNA-seq data (Fig 10), confirming the efficiency and accuracy of the RNA-seq experiments.
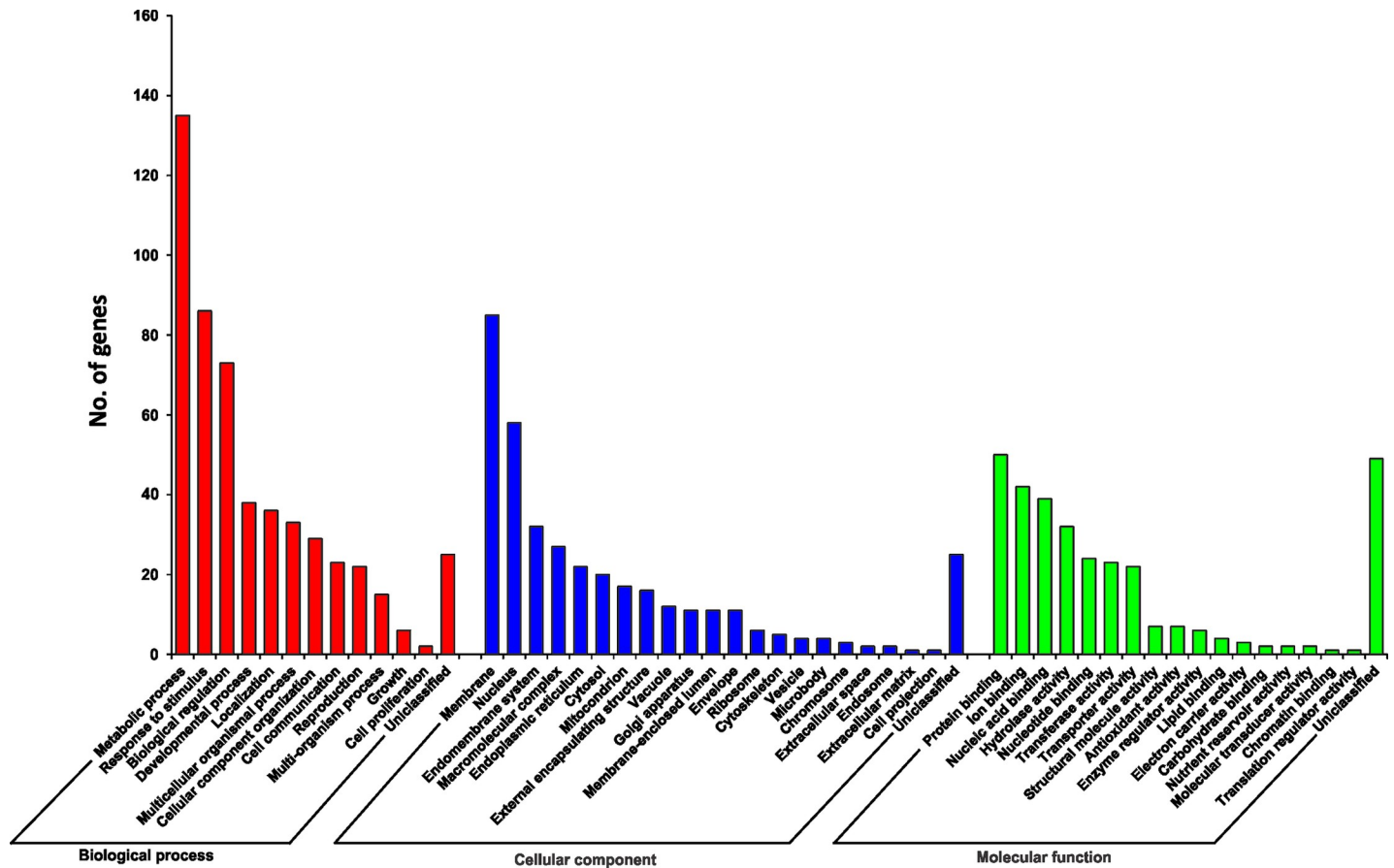
Fig 5. Gene ontology (GO) classification of differentially expressed genes between normal (N) and stunted (S) cherry tomato plants (cv. 'Minichal').

Discussion

Deep sequencing-based RNA-seq technology has made it possible to rapidly analyze large genomic datasets and quantify transcriptomes [33]. This high-throughput, next-generation sequencing technology has become a powerful tool for analyzing transcriptomes, and has been successfully used for both human and plant transcriptomes [34]. Global gene expression patterns can be determined using RNA-seq in samples of tissues at different developmental stages, with contrasting characteristics, or in response to different environmental stimuli [33,35,36]. In this study, we observed a stunted phenotype of the cherry tomato cv. 'Minichal', which is characterized by alterations in plant height, leaf size/shape, and fruit size/shape compared to the normal phenotype. We used RNA-seq to profile the transcriptomes of normal (N) and stunted (S) cherry tomatoes of this cultivar. We obtained almost 115.450 million high-quality clean reads, which were assembled into 35,216 transcripts (Table 1).

Our results identified 661 DEGs between the pooled RNA of N and S tomato plants (S2 Table). Subsequently, GO enrichment revealed that 'metabolic process' and 'catalytic activity' were the most enriched GO terms for both up-regulated and down-regulated genes between N and S (S3 Table).

To obtain further insight into the biological functions of these DEGs, GO functional annotation and KEGG pathway enrichment analysis were performed using the DAVID tool. Functional annotation clustering of DEGs revealed that the most enriched GO terms were associated with the sterol biosynthesis process (GO:0016126; enrichment score 2.37) (Table 2).
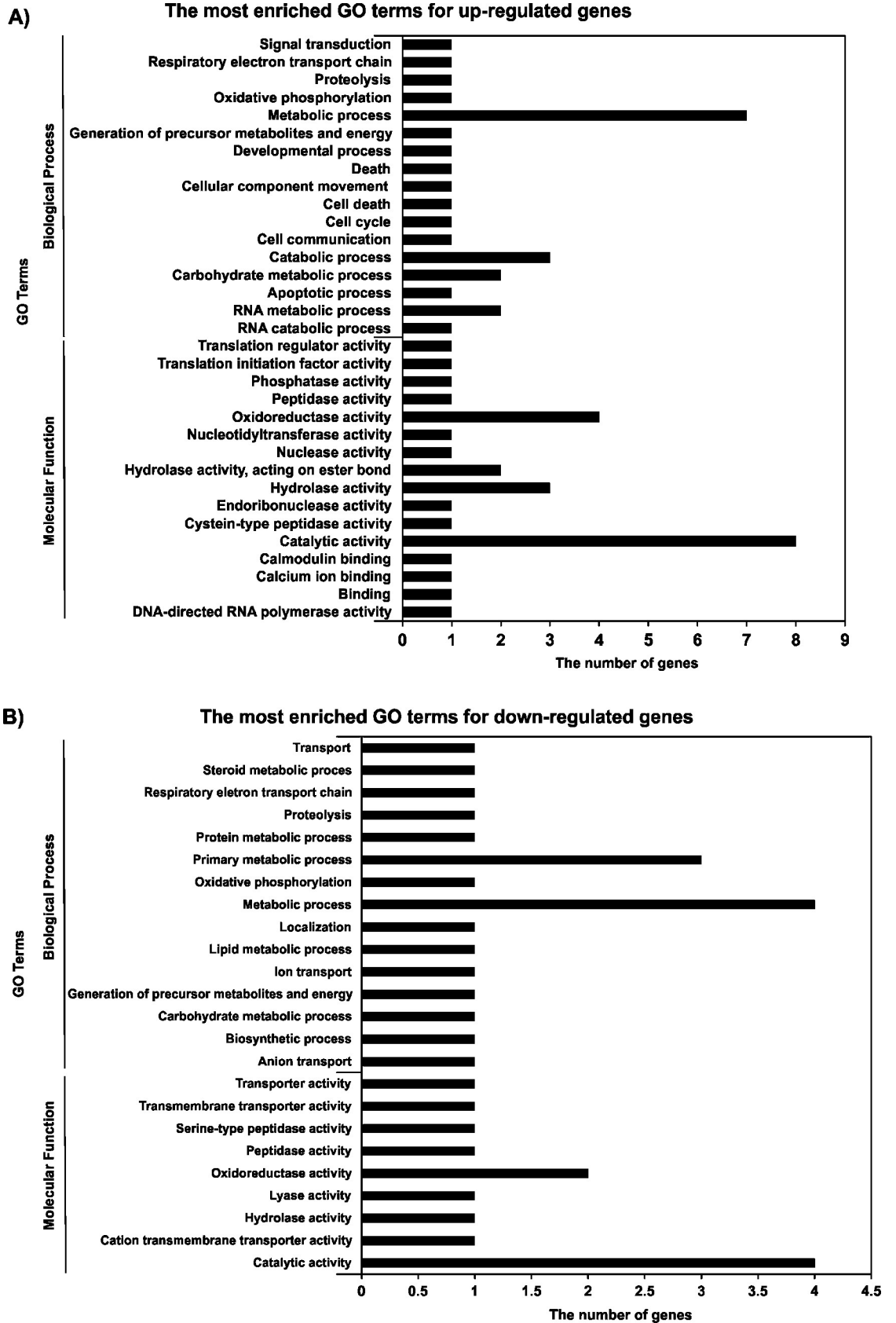
A)

The most enriched GO terms for up-regulated genes

B)

The most enriched GO terms for down-regulated genes

Fig 6. GO enrichment of up-regulated (A) and down-regulated (B) genes in leaves of stunted (S) and normal (N) cherry tomato plants (cv. 'Minichal'). The P-value was corrected as $P < 0.5$.

KEGG pathway enrichment also indicated that 'steroid biosynthesis' and 'homologous recombination' were the most enriched pathways (Table 3). These results clearly suggest that genes related to steroid biosynthesis might be involved in dwarfism in S tomatoes.

Several studies have been conducted on plant dwarfism. Dwarfism is sometimes advantageous; for example in cereal crops—specifically rice and wheat, where lodging decreases crop productivity [37]. However, in tomato, dwarfism is deleterious because it reduces both quality and productivity. Plant dwarfism results from many genetic defects, mostly associated with hormone biosynthesis and perception [12]. Functional analysis of several genes related to dwarfism has previously been reported, including genes related to BR and GA biosynthesis and perception in different plant species [22,28,38–41].

BRs play significant roles in plant growth and development, and are biosynthesized via multiple parallel pathways starting with the precursor campesterol [15,24,42,43]. Defects in the BR biosynthesis/signaling cause dwarfism in plants [13]. For example, in *Arabidopsis*, *dwarf5* (*dwf5*) mutants have a mutation in the gene for the enzyme 7-dehydrocholesterol reductase, which disrupts the sterol Δ^7 reduction step and leads to dwarfism [25]. Likewise in *Arabidopsis*,

Table 2. Functional annotation clustering of differentially expressed genes (DEGs).

Category	Term	Count	P-value	Fold enrichment	Benjamini	FDR
Annotation cluster 1 (enrichment score: 2.37)						
UP_KEYWORDS	Sterol metabolism	4	0.002	15.289	0.052	2.723
UP_KEYWORDS	Sterol biosynthesis	4	0.002	15.289	0.052	2.723
UP_KEYWORDS	Steroid biosynthesis	4	0.007	10.084	0.096	8.651
GOTERM_BP_DIRECT	GO:0016126~sterol biosynthetic process	4	0.010	9.024	0.715	12.631
Annotation cluster 2 (enrichment score: 1.39)						
SMART	SM00774:WRKY	4	0.029	5.923	0.769	24.581
INTERPRO	IPR003657:DNA-binding WRKY	4	0.034	5.608	0.987	38.225
UP_SEQ_FEATURE	DNA-binding region:WRKY	4	0.069	4.179	0.998	62.629
Annotation cluster 3 (enrichment score: 1.25)						
UP_KEYWORDS	DNA repair	5	0.031	4.232	0.188	32.221
UP_KEYWORDS	DNA damage	5	0.037	4.003	0.203	37.264
GOTERM_BP_DIRECT	GO:0006281~DNA repair	5	0.157	2.384	0.963	90.610
Annotation cluster 4 (enrichment score: 1.18)						
UP_KEYWORDS	TPR repeat	4	0.0212	6.7709	0.1591	23.4605
INTERPRO	IPR019734:Tetratricopeptide repeat	4	0.1040	3.5289	0.9970	77.9970
INTERPRO	IPR013026:Tetratricopeptide repeat-containing domain	4	0.1269	3.2232	0.9962	84.6116
Annotation cluster 5 (enrichment score: 1.17)						
UP_SEQ_FEATURE	domain:MADS-box	4	0.025	6.322	0.988	28.834
SMART	SM00432:MADS	4	0.067	4.223	0.823	48.634
INTERPRO	IPR002100:Transcription factor, MADS-box	4	0.090	3.756	0.997	72.901
GOTERM_BP_DIRECT	GO:0045944~positive regulation of transcription from RNA polymerase II promoter	4	0.147	3.008	0.961	88.971
Annotation cluster 6 (enrichment score: 1.07)						
INTERPRO	IPR002487:Transcription factor, K-box	3	0.058	7.675	0.996	55.937
UP_SEQ_FEATURE	domain:K-box	3	0.074	6.604	0.996	65.226
GOTERM_BP_DIRECT	GO:0000165~MAPK cascade	3	0.144	4.476	0.976	88.369

Table 3. KEGG pathway enrichment of differentially expressed genes between N and S.

Sl. no.	Pathway name	No. of genes	*P*-value	Benjamini
1	ath00100:Steroid biosynthesis	3	0.056	0.794
2	ath03440:Homologous recombination	4	0.025	0.748
3	ath03430:Mismatch repair	3	0.071	0.741
4	ath03030:DNA replication	3	0.109	0.795
5	ath03060:Protein export	3	0.116	0.743
6	ath00966:Glucosinolate biosynthesis	2	0.127	0.714
7	ath00750:Vitamin B6 metabolism	2	0.147	0.714
8	ath03420:Nucleotide excision repair	3	0.183	0.750
9	ath01210:2-Oxocarboxylic acid metabolism	3	0.203	0.750
10	ath00908:Zeatin biosynthesis	2	0.203	0.714
11	ath00073:Cutin, suberin and wax biosynthesis	2	0.265	0.785

https://doi.org/10.1371/journal.pone.0208770.t003

dwarfism occurs in *dwf4* mutants, which have a mutation in the gene encoding steroid 22α hydroxylase (CYP90B1), which is involved in 22α-hydroxylation of the BR pathway [24].

In this study, three DEGs, *3beta-hydroxysteroid-dehydrogenase* (*3BETAHSD/D2*, Solyc02g081730.2), *7-dehydrocholesterol reductase* (*DWF5*, Solyc06g074090.2), and *delta(24)-sterol reductase* (*DIM*, Solyc02g069490.2)—all related to the steroid hormone biosynthesis pathway—were down-regulated in S compared to N plants (Figs 7 and 10). We also checked the expression patterns of these three genes in leaf, inflorescence, and fruit tissues of the cherry tomato cv. 'Minichal' (Fig 11). The result indicated that the expression of these steroid biosynthesis genes was higher in N than S plants. In N, expression was highest in leaf and lowest in fruit, while in S, expression was similar in leaves and inflorescences, but was drastically reduced in fruits.

The protein interaction network of three steroid biosynthesis-related genes, *3beta-hydroxysteroid-dehydrogenase* (*3BETAHSD/D2*), *7-dehydrocholesterol reductase* (*DWF5*), and *delta (24)-sterol reductase* (*DIM*), highlighted their possible contribution to dwarfism of tomato plants (Fig 12). In S cherry tomatoes, these genes might be involved in dwarfism by directly or indirectly affecting steroid biosynthesis. In apple plants (*Malus × domestica*), colchicine-induced autotetraploid plants showed dwarfism, with decreased levels of indole-3-acetic acid (IAA) and BR compared to diploid plants. Furthermore, digital gene expression analysis of these apple plants revealed that DEGs between them were mostly related to IAA and BR biosynthesis pathways [44]. In *Arabidopsis*, a biosynthetic defect in *dwf1*, which encodes *delta (24)-sterol reductase*, resulted in dwarfism with reduced levels of BR synthesis compared to the wild type [45]. A similar *dwf1* dwarf mutant has been reported in pea [46]. The *dwf5* mutant, which is defective in BR biosynthesis, also showed a dwarf phenotype in *Arabidopsis* [25]. In rice, the dwarf mutant *ebisu dwarf* (*d2*) is deficient in BR biosynthesis and caused dwarfism, but exogenous application of BL restored the normal phenotype [39]. In tomato, the BR biosynthesis-defective mutant *Dwarf* (*D*), which harbors a mutation in *cytochrome P450* (*P450*), exhibits dwarfism, while complementation *35S::D* lines restore the normal phenotype [12,40]. Similar dwarf mutant *dumpy* (*dpy*) resulted from the mutation of mutation in the *C-23 steroid hydroxylase* (*cpd*) gene has also been reported in tomato by Kaka et al. [47]. However, our reported genes (*3BETAHSD/D2*, *DWF5* and *DIM*) for dwarfism of cherry tomato are different from those previously reported mutants like *D* and *dpy*. Up-regulation of *cytokinin dehydrogenase 3* (*CKX3*) in S tomatoes led to a higher rate of cytokinin degradation in these plants. Reid et al. [48] reported that the cytokinin content was negatively regulated by the activity of *CKX3* in the root of *Lotus japonicus ckx3* mutants.

The auxin signaling genes *AIR12 (Solyc09g056390.1)*, and *AXX15 (Solyc04g053000.1)*, but not *IAA14*, were down-regulated in N ([Fig 8](#)). This suggests that auxin signaling genes might be affected, leading to defective plant development. A similar result has been reported in tetraploid apple [44].

Gene Accession	Gene Name	Description	N	S
Steroid biosynthesis				
Solyc02g081730.2	*3BETAHSD/D2*	3beta-hydroxysteroid-dehydrogenase/decarboxylase isoform 2	76.808	49.463
Solyc06g074090.2	*DWF5*	7-dehydrocholesterol reductase	191.153	121.712
Solyc02g069490.2	*DIM*	Delta(24)-sterol reductase	552.388	302.667
Homologous recombination				
Solyc09g009900.2	*RPA3B*	Replication protein A 14 kDa subunit B	8.604	18.009
Solyc10g081830.1	*RPA2B*	Replication protein A 32 kDa subunit B	14.188	28.248
Solyc07g055170.1	*XRCC3*	DNA repair protein XRCC3 homolog	0.000	0.840
Solyc03g013260.1	*RPA1E*	Replication protein A 70 kDa DNA-binding subunit E	0.000	1.551
Mismatch repair				
Solyc10g081830.1	*RPA2B*	Replication protein A 32 kDa subunit B	14.188	28.248
Solyc09g009900.2	*RPA3B*	Replication protein A 14 kDa subunit B	8.604	18.009
Solyc03g013260.1	*RPA1E*	Replication protein A 70 kDa DNA-binding subunit E	0.000	1.551
DNA replication				
Solyc10g081830.1	*RPA2B*	Replication protein A 32 kDa subunit B	14.188	28.248
Solyc09g009900.2	*RPA3B*	Replication protein A 14 kDa subunit B	8.604	18.009
Solyc03g013260.1	*RPA1E*	Replication protein A 70 kDa DNA-binding subunit E	0.000	1.551
Protein export				
Solyc03g005740.1	*SPase 12 kDa subunit*	Probable signal peptidase complex subunit 1	3536.440	570.896
Solyc06g010060.1	*SC61B_ARATH*	Protein transport protein Sec61 subunit beta	76.229	36.458
Solyc12g099820.1	*SRP9*	Signal recognition particle 9 kDa protein	169.084	77.856
Glucosinolate biosynthesis				
Solyc09g092580.2	*CYP83B1*	Cytochrome P450 83B1	26.271	14.735
Solyc05g006140.1	*UGT74B1*	UDP-glycosyltransferase 74B1	9.635	4.226
Vitamin B6 metabolism				
Solyc06g062550.2	*PPSP2_ARATH*	Inorganic pyrophosphatase 2	1.544	8.074
Solyc06g062540.2	*PS2*	Inorganic pyrophosphatase 1	9.053	55.520
Nucleotide excision repair				
Solyc10g081830.1	*RPA2B*	Replication protein A 32 kDa subunit B	14.188	28.248
Solyc09g009900.2	*RPA3B*	Replication protein A 14 kDa subunit B	8.604	18.009
Solyc03g013260.1	*RPA1E*	Replication protein A 70 kDa DNA-binding subunit E	0.000	1.551
Oxocarboxylic acid metabolism				
Solyc09g092580.2	*CYP83B1*	Cytochrome P450 83B1	26.271	14.735
Solyc05g006140.1	*UGT74B1*	UDP-glycosyltransferase 74B1	9.635	4.226
Solyc06g063090.2	*ALAAT2*	Alanine aminotransferase 2, mitochondrial	8.241	13.640
Zeatin biosynthesis				
Solyc09g064910.1	*IPT3*	Adenylate isopentenyltransferase 3, chloroplastic	0.000	0.675
Solyc12g008900.1	*CKX3*	Cytokinin dehydrogenase 3	0.381	3.286
Cutin, suberine and wax biosynthesis				
Solyc01g088400.2	*CER1*	Protein ECERIFERUM 1	33.813	21.426
Solyc03g121600.2	*HTH*	Protein HOTHEAD	30.668	20.104

Fig 7. Heatmap illustration of the expression of genes involved in homologous recombination and steroid biosynthesis in normal (N) and stunted (S) cherry tomatoes of the cultivar 'Minichal'. FPKM values were obtained from RNA-seq data. Red and blue colors represent the maximum and the minimum values, respectively.

Gene Accession	Gene Name	Description	N	S
Auxin signaling pathway				
Solyc09g056390.1	AIR12	Auxin-induced in root cultures protein 12	631.394	96.683
Solyc09g083290.2	IAA14	Auxin-responsive protein IAA14	119.289	187.353
Solyc04g053000.1	AXX15_SOYBN	Auxin-induced protein X15	17.112	0.000
Solyc04g053010.1	AX6B_SOYBN	Auxin-induced protein 6B	0.000	2.972
Solyc11g011650.1	AXX15_SOYBN	Auxin-induced protein X15	0.000	3.718
Solyc02g077880.2	12KD_FRAAN	Auxin-repressed 12.5 kDa protein	83.182	235.683
Ethylene biosynthesis and signaling perception				
Solyc07g049530.2	ACO1	1-aminocyclopropane-1-carboxylate oxidase 1	32.688	52.294
Solyc09g089580.2	ACO3	1-aminocyclopropane-1-carboxylate oxidase homolog	7.108	14.822
Solyc01g090310.2	ERF13	Ethylene-responsive transcription factor 13	0.000	0.609
Solyc01g090340.2	ERF13	Ethylene-responsive transcription factor 13	153.225	98.785
Solyc03g093560.1	ERF5	Ethylene-responsive transcription factor 5	2.373	6.513
Solyc03g117130.2	ERF003	Ethylene-responsive transcription factor ERF003	0.000	0.900

Fig 8. Heatmap illustration of the expression of auxin and ethylene signaling perception genes in normal (N) and stunted (S) cherry tomatoes of the cultivar 'Minichal'. FPKM values were obtained from RNA-seq data. Red and blue colors represent the maximum and minimum values, respectively.

Previous studies have revealed that GA has an effect on plant growth and development. For example, exogenous treatment of dwarf pea and dwarf maize seedlings with GA3 enhanced longitudinal growth rates [49]. However, we found no DEGs related to GA biosynthesis in this study.

Gene Accession	Gene Name	Description	N	S
WRKY				
Solyc01g095630.2	WRKY41	Probable WRKY transcription factor 41	21.617	35.610
Solyc03g116890.2	WRKY40	Probable WRKY transcription factor 40	0.957	2.668
Solyc12g056750.1	WRKY51	Probable WRKY transcription factor 51	0.000	0.667
Solyc08g062490.2	WRKY50	Probable WRKY transcription factor 50	3.899	8.566
MADS-box				
Solyc01g103550.1	AGL36	Agamous-like MADS-box protein AGL36	0.000	0.729
Solyc04g076280.2	SVP	MADS-box protein SVP	20.431	10.529
Solyc08g080100.2	AGL19	Agamous-like MADS-box protein AGL19	16.312	9.399
Solyc02g089200.2	SEPALLATA 2	Developmental protein SEPALLATA 2	0.251	10.539
MAPK				
Solyc06g036080.2	YDA	Mitogen-activated protein kinase kinase kinase YODA	16.198	10.702
TPR				
Solyc10g078250.1	FKBP65	FKBP-type peptidyl-prolyl cis-trans isomerase family protein	100.941	28.278
Solyc06g007970.2	ATSDI1	Tetratricopeptide repeat (TPR)-like superfamily protein	1.185	6.088
Solyc09g063140.2	LPA1	Tetratricopeptide repeat (TPR)-containing protein	38.536	35.080
Solyc05g050630.2	NOXY38	Tetratricopeptide repeat (TPR)-containing protein	20.482	13.405

Fig 9. Heatmap illustration of the expression of WRKY, MADS-box, MAPK, and TRP TFs in normal (N) and stunted (S) cherry tomatoes of the cultivar 'Minichal'. FPKM values were obtained from RNA-seq data. Red and blue colors represent the maximum and minimum values, respectively.
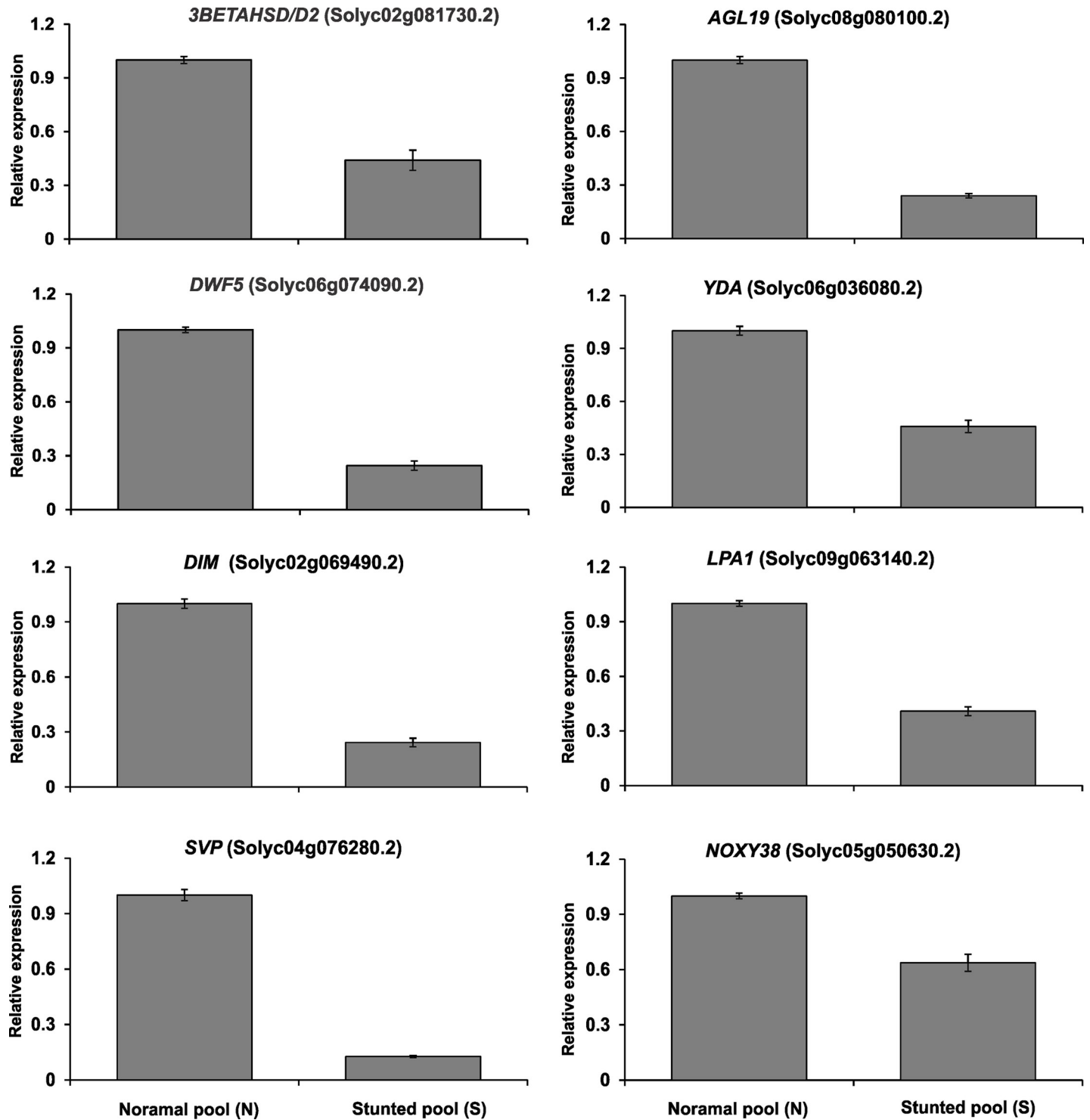
Fig 10. Validation of differentially expressed genes between normal (N) and stunted (S) cherry tomatoes of the cultivar 'Minichal' by qRT-PCR. Error bar indicates ±SE of the means of three replicates.

The up-regulation of two *1-aminocyclopropane-1-carboxylic acid oxidase* genes, *ACO1* and *ACO3*, which are involved in the final step of ethylene biosynthesis, suggests higher levels of
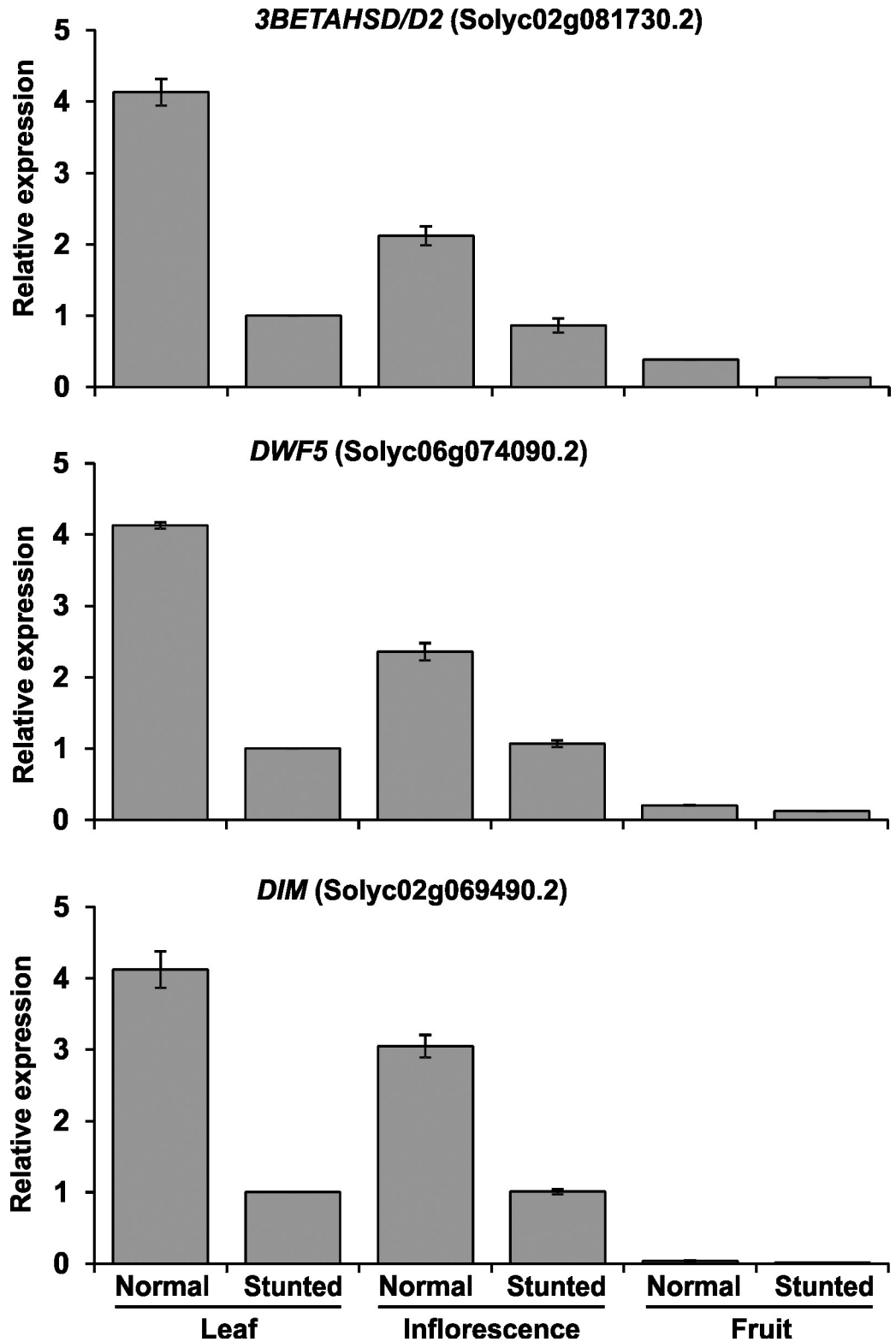
Fig 11. Relative expression of three genes related to steroid biosynthesis in leaf, inflorescence, and fruit of normal (N) and stunted (S) plants of the cherry tomato cv. 'Minichal'. Error bar indicates ±SE of the means of three replicates.
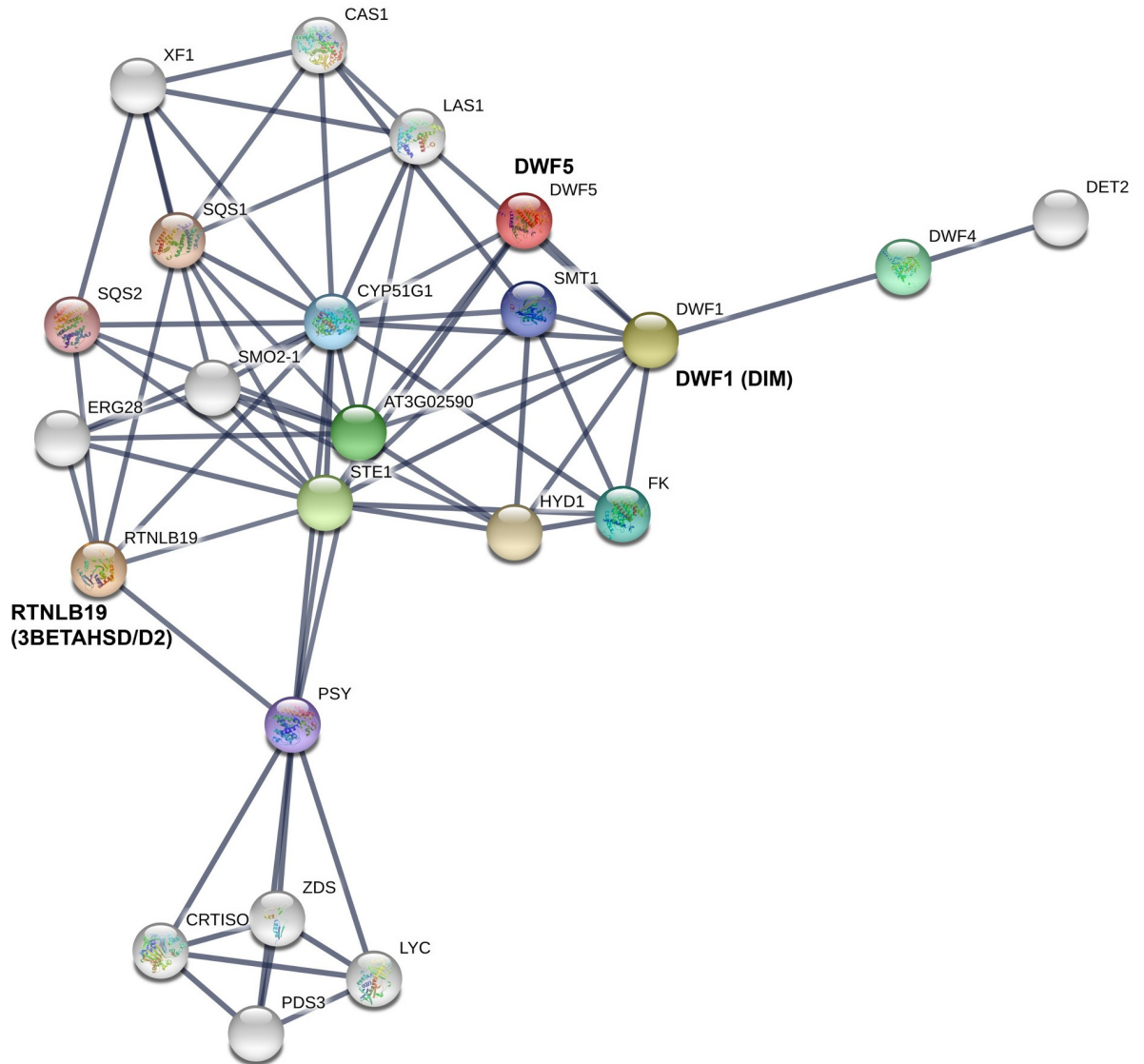
Fig 12. Protein network interaction of differentially expressed steroid pathway-related genes and proteins analyzed using STRING (http://string.embl.de).

https://doi.org/10.1371/journal.pone.0208770.g012

ethylene production in S tomatoes, which might affect plant growth and development. Ethylene overproduction has been shown to inhibit plant growth in *Arabidopsis* [50,51].

The 'short vegetative phase' (SVP) group of MADS-box genes, such as *OsMADS22*, *OsMADS47*, and *OsMADS55*, have been shown to act as negative regulators of BR responses in rice [52]. The double and triple RNAi plants (*OsMADS22–OsMADS55* and *OsMADS22–OsMADS47–OsMADS55*, respectively) showed reduced stem elongation. Unexpectedly, in this study, we also found that the expression of the MADS-box genes *SVP* (*Solyc04g076280.2*) and *AGL19* (*Solyc08g080100.2*) was down-regulated, and *AGL36* (*Solyc01g103550.1*) and *SEPAL-LATA2* (*Solyc02g089200.2*) were up-regulated in S compared to N plants (Fig 9). Overexpression of *OsMADS1* causes dwarfism in rice via irregular activation of BR and GA synthesis pathways [53].

Kim et al. [54] demonstrated that BR controls stomatal development by activating *mitogen-activated protein kinase kinase kinase* (*MAPKKK*) in *Arabidopsis*. Likewise, we found that *MAPKK* was up-regulated in S compared to N tomatoes (Fig 9).

Conclusions

We conducted comparative transcriptome analysis using normal and stunted plants of the cherry tomato cv. 'Minichal'. DEGs related to steroid biosynthesis may be involved in dwarfism in this tomato cultivar. To best of our knowledge, this is the first comparative transcriptome analysis for plant dwarfism in tomato. Our results provide insight into the molecular mechanism of dwarfism and lay the foundation for future studies in related species.

Supporting information

S1 Table. Primers used for qRT-PCR validation.
(XLSX)

S2 Table. Differentially expressed genes between normal (N) and stunted (S) tomato plants.
(XLSX)

S3 Table. GO terms overrepresented in up-regulated and down-regulated genes, and number of genes belonging to each term.
(XLSX)

S4 Table. Twenty-two functional annotation clusters of DEGs.
(XLSX)

Acknowledgments

Author Contributions

Conceptualization: Ill-Sup Nou.

Data curation: Md Abdur Rahim.

Formal analysis: Md Abdur Rahim, Hee-Jeong Jung.

Funding acquisition: Ill-Sup Nou.

Investigation: Md Abdur Rahim, Hee-Jeong Jung, Khandker Shazia Afrin.

Methodology: Md Abdur Rahim, Hee-Jeong Jung.

Project administration: Ill-Sup Nou.

Resources: Ill-Sup Nou.

Validation: Md Abdur Rahim, Hee-Jeong Jung, Khandker Shazia Afrin, Ji-Hee Lee.

Writing – original draft: Md Abdur Rahim.

Writing – review & editing: Md Abdur Rahim, Ill-Sup Nou.

References

1. Foolad MR. Genome mapping and molecular breeding of tomato. Int J Plant Genomics. 2007; 2007: 64358. https://doi.org/10.1155/2007/64358 PMID: 18364989

2. Müller L, Caris-Veyrat C, Lowe G, Böhm V. Lycopene and its antioxidant role in the prevention of cardio-vascular diseases—a critical review. Crit Rev Food Sci Nutr. 2016; 56:1868–1879. https://doi.org/10.1080/10408398.2013.801827 PMID: 25675359

3. Burton-Freeman BM, Sesso HD. Whole food versus supplement: comparing the clinical evidence of tomato intake and lycopene supplementation on cardiovascular risk factors. Adv Nutr An Int Rev J. 2014; 5:457–485. https://doi.org/10.3945/an.114.005231 PMID: 25469376

4. Holick CN, Michaud DS, Stolzenberg-Solomon R, Mayne ST, Pietinen P, Taylor PR, et al. Dietary carot-enoids, serum beta-carotene, and retinol and risk of lung cancer in the alpha-tocopherol, beta-carotene cohort study. Am J Epidemiol. 2002; 156:536–47. https://doi.org/10.1093/aje/kwf072 PMID: 12226001

5. Holzapfel NP, Holzapfel BM, Champ S, Feldthusen J, Clements J, Hutmacher DW. The potential role of lycopene for the prevention and therapy of prostate cancer: From molecular mechanisms to clinical evi-dence. Int J Mol Sci. 2013; 4(7):14620–14646. https://doi.org/10.3390/ijms140714620

6. Erge HS, Karadeniz F. Bioactive compounds and antioxidant activity of tomato cultivars. Int J Food Prop. 2011; 14:968–977. https://doi.org/10.1080/10942910903506210

7. Ilahy R, Hdider C, Lenucci MS, Tlili I, Dalessandro G. Phytochemical composition and antioxidant activ-ity of high-lycopene tomato (*Solanum lycopersicum* L.) cultivars grown in Southern Italy. Sci Hortic. 2011; 127:255–261. https://doi.org/10.1016/j.scienta.2010.10.001

8. Ranc N, Muños S, Santoni S, Causse M. A clarified position for *Solanum lycopersicum* var. *cerasiforme* in the evolutionary history of tomatoes (Solanaceae). BMC Plant Biol. 2008; 8:130. https://doi.org/10.1186/1471-2229-8-130 PMID: 19099601

9. Choi SH, Kim HR, Kim HJ, Lee IS, Kozukue N, Levin CE, et al. Free amino acid and phenolic contents and antioxidative and cancer cell-inhibiting activities of extracts of 11 greenhouse-grown tomato varie-ties and 13 tomato-based foods. J Agric Food Chem. 2011; 59:12801–12814. https://doi.org/10.1021/jf202791j PMID: 22070764

10. Koornneef M, van der Veen JH. Induction and analysis of gibberellin sensitive mutants in *Arabidopsis thaliana* (L.) heynh. Theor Appl Genet. 1980; 58:257–263. https://doi.org/10.1007/BF00265176 PMID: 24301503

11. Timpte CS, Wilson AK, Estelle M. Effects of the axr2 mutation of *Arabidopsis* on cell shape in hypocotyl and inflorescence. Planta. 1992; 188:271–278. https://doi.org/10.1007/BF00216824 PMID: 24178265

12. Bishop GJ, Nomura T, Yokota T, Harrison K, Noguchi T, Fujioka S, et al. The tomato DWARF enzyme catalyses C-6 oxidation in brassinosteroid biosynthesis. Proc Natl Acad Sci U S A. 1999; 96:1761–1766. https://doi.org/10.1073/pnas.96.4.1761 PMID: 9990098

13. Chung Y, Choe S. The regulation of brassinosteroid biosynthesis in *Arabidopsis*. Crit Rev Plant Sci. 2013; 32:396–410. https://doi.org/10.1080/07352689.2013.797856

14. Fujioka S, Sakurai A. Brassinosteroids. Nat Prod Rep. 1997; 14:1–10. Available: http://pubs.rsc.org/en/Content/ArticlePDF/1997/NP/NP9971400001 PMID: 9121728

15. Shimada Y, Fujioka S, Miyauchi N, Kushiro M, Takatsuto S, Nomura T, et al. Brassinosteroid-6-oxi-dases from *Arabidopsis* and tomato catalyze multiple C-6 oxidations in brassinosteroid biosynthesis. Plant Physiol. 2001; 126:770–779. https://doi.org/10.1104/pp.126.2.770 PMID: 11402205

16. Grove MD, Spencer GF, Rohwedder WK, Mandava N, Worley JF, Warthen JD, et al. Brassinolide, a plant growth-promoting steroid isolated from *Brassica napus* pollen. Nature. 1979; 281:216–217. https://doi.org/10.1038/281216a0

17. Clouse SD, Sasse JM. BRASSINOSTEROIDS: Essential regulators of plant growth and development. Annu Rev Plant Physiol Plant Mol Biol. 1998; 49: 427–451. https://doi.org/10.1146/annurev.arplant.49.1.427 PMID: 15012241

18. Nomura T, Jager CE, Kitasaka Y, Takeuchi K, Fukami M, Yoneyama K, et al. Brassinosteroid deficiency due to truncated steroid 5alpha-reductase causes dwarfism in the lk mutant of pea. Plant Physiol. 2004; 135:2220–9. https://doi.org/10.1104/pp.104.043786 PMID: 15286289

19. Li J, Nagpal P, Vitart V, McMorris TC, Chory J. A role for brassinosteroids in light-dependent develop-ment of Arabidopsis. Science. 1996; 272:398–401. https://doi.org/10.1126/science.272.5260.398 PMID: 8602526

20. Klahre U, Noguchi T, Fujioka S, Takatsuto S, Yokota T, Nomura T, et al. The *Arabidopsis DIMINUTO/DWARF1* gene encodes a protein involved in steroid synthesis. Plant Cell. 1998; 10:1677–90. Avail-able: http://www.ncbi.nlm.nih.gov/pubmed/9761794 PMID: 9761794

21. Kauschmann A, Jessop A, Koncz C, Szekeres M, Willmitzer L, Altmann T. Genetic evidence for an essential role of brassinosteroids in plant development. Plant J. 1996; 9:701–713. https://doi.org/10.1046/j.1365-313X.1996.9050701.x

22. Szekeres M, Németh K, Koncz-Kálmán Z, Mathur J, Kauschmann A, Altmann T, et al. Brassinosteroids rescue the deficiency of CYP90, a cytochrome P450, controlling cell elongation and de-etiolation in Arabidopsis. Cell. 1996; 85:171–182. https://doi.org/10.1016/S0092-8674(00)81094-6 PMID: 8612270

23. Azpiroz R. An Arabidopsis brassinosteroid-dependent mutant is blocked in cell elongation. Plant Cell. 1998; 10:219–230. https://doi.org/10.1105/tpc.10.2.219 PMID: 9490745

24. Choe S, Dilkes BP, Fujioka S, Takatsuto S, Sakurai A, Feldmann K a. The DWF4 gene of Arabidopsis encodes a cytochrome P450 that mediates multiple 22alpha-hydroxylation steps in brassinosteroid biosynthesis. Plant Cell. 1998; 10:231–43. https://doi.org/10.1105/tpc.10.2.231 PMID: 9490746

25. Choe S, Tanaka A, Noguchi T, Fujioka S, Takatsuto S, Ross AS, et al. Lesions in the sterol Δ7reductase gene of Arabidopsis cause dwarfism due to a block in brassinosteroid biosynthesis. Plant J. 2000; 21:431–443. https://doi.org/10.1046/j.1365-313X.2000.00693.x PMID: 10758495

26. Choe S, Noguchi T, Fujioka S, Takatsuto S, Tissier CP, Gregory BD, et al. The Arabidopsis dwf7/ste1 mutant is defective in the delta7 sterol C-5 desaturation step leading to brassinosteroid biosynthesis. Plant Cell. American Society of Plant Biologists; 1999; 11:207–221. https://doi.org/10.1105/TPC.11.2.207

27. Ephritikhine G, Pagant S, Fujioka S, Takatsuto S, Lapous D, Caboche M, et al. The sax1 mutation defines a new locus involved in the brassinosteroid biosynthesis pathway in Arabidopsis thaliana. Plant J. 1999; 18:315–320. https://doi.org/10.1046/j.1365-313X.1999.00455.x PMID: 10377996

28. Hong Z, Ueguchi-Tanaka M, Shimizu-Sato S, Inukai Y, Fujioka S, Shimada Y, et al. Loss-of-function of a rice brassinosteroid biosynthetic enzyme, C-6 oxidase, prevents the organized arrangement and polar elongation of cells in the leaves and stem. Plant J. 2002; 32:495–508. https://doi.org/10.1046/j.1365-313X.2002.01438.x PMID: 12445121

29. Trapnell C, Roberts A, Goff L, Pertea G, Kim D, Kelley DR, et al. Differential gene and transcript expression analysis of RNA-seq experiments with TopHat and Cufflinks. Nat Protoc. 2012; 7:562–578. https://doi.org/10.1038/nprot.2012.016 PMID: 22383036

30. Wang L, Feng Z, Wang X, Wang X, Zhang X. DEGseq: an R package for identifying differentially expressed genes from RNA-seq data. Bioinformatics. 2010; 26: 136–138. https://doi.org/10.1093/bioinformatics/btp612 PMID: 19855105

31. Wang J, Duncan D, Shi Z, Zhang B. WEB-based GEne SeT AnaLysis Toolkit (WebGestalt): update 2013. Nucleic Acids Res. 2013; 41:W77–W83. https://doi.org/10.1093/nar/gkt439 PMID: 23703215

32. Livak KJ, Schmittgen TD. Analysis of relative gene expression data using real-time quantitative PCR and the 2-ΔΔCT method. Methods. 2001; 25:402–408. https://doi.org/10.1006/meth.2001.1262 PMID: 11846609

33. Wang Z, Gerstein M, Snyder M. RNA-Seq: a revolutionary tool for transcriptomics. Nat Rev Genet. 2009; 10:57–63. https://doi.org/10.1038/nrg2484 PMID: 19015660

34. Lu T, Lu G, Fan D, Zhu C, Li W, Zhao Q, et al. Function annotation of the rice transcriptome at single-nucleotide resolution by RNA-seq. Genome Res. 2010; 20:1238–1249. https://doi.org/10.1101/gr.106120.110 PMID: 20627892

35. Mortazavi A, Williams BA, McCue K, Schaeffer L, Wold B. Mapping and quantifying mammalian transcriptomes by RNA-Seq. Nat Methods. 2008; 5:621–628. https://doi.org/10.1038/nmeth.1226 PMID: 18516045

36. Miao X, Luo Q. Genome-wide transcriptome analysis between small-tail Han sheep and the Surabaya fur sheep using high-throughput RNA sequencing. Reproduction. 2013; 145:587–96. https://doi.org/10.1530/REP-12-0507 PMID: 23579189

37. Kovi MR, Zhang Y, Yu S, Yang G, Yan W, Xing Y. Candidacy of a chitin-inducible gibberellin-responsive gene for a major locus affecting plant height in rice that is closely linked to Green Revolution gene sd1. Theor Appl Genet. 2011; 123:705–714. https://doi.org/10.1007/s00122-011-1620-x PMID: 21637999

38. Ueguchi-Tanaka M, Ashikari M, Nakajima M, Itoh H, Katoh E, Kobayashi M, et al. GIBBERELLIN INSENSITIVE DWARF1 encodes a soluble receptor for gibberellin. Nature. 2005; 437:693–698. https://doi.org/10.1038/nature04028 PMID: 16193045

39. Hong Z, Ueguchi-Tanaka M, Umemura K, Uozu S, Fujioka S, Takatsuto S, et al. A rice brassinosteroid-deficient mutant, ebisu dwarf (d2), is caused by a loss of function of a new member of cytochrome P450. Plant Cell. 2003; 15:2900–2910. https://doi.org/10.1105/tpc.014712 PMID: 14615594

40. Bishop GJ, Harrison K, Jones JD. The tomato Dwarf gene isolated by heterologous transposon tagging encodes the first member of a new cytochrome P450 family. Plant Cell. 1996; 8:959–969. https://doi.org/10.1105/Tpc.8.6.959 PMID: 8672892

41. Schultz L, Kerckhoffs LHJ, Klahre U, Yokota T, Reid JB. Molecular characterization of the brassinoster-oid-deficient lkb mutant in pea. Plant Mol Biol. 2001; 47:491–498. https://doi.org/10.1023/A:1011894812794 PMID: 11669574

42. Fujioka S, Choi YH, Takatsuto S, Yokota T, Li J, Chory J, et al. Identification of castasterone, 6-deoxo-castasterone, typhasterol and 6-deoxotyphasterol from the shoots of *Arabidopsis thaliana*. Plant Cell Physiol. 1996; 37:1201–1203. https://doi.org/10.1093/oxfordjournals.pcp.a029074 PMID: 9032971

43. Choi YH, Fujioka S, Nomura T, Harada A, Yokota T, Takatsuto S, et al. An alternative brassinolide bio-synthetic pathway via late C-6 oxidation. Phytochemistry. 1997; 44:609–613. https://doi.org/10.1016/S0031-9422(96)00572-9

44. Ma Y, Xue H, Zhang L, Zhang F, Ou C, Wang F, et al. Involvement of auxin and brassinosteroid in dwarfism of autotetraploid apple (*Malus × domestica*). Sci Rep. 2016; 6:26719. https://doi.org/10.1038/srep26719 PMID: 27216878

45. Choe S, Dilkes BP, Gregory BD, Ross AS, Yuan H, Noguchi T, et al. The Arabidopsis dwarf1 mutant is defective in the conversion of 24-methylenecholesterol to campesterol in brassinosteroid biosynthesis. Plant Physiol. 1999; 119:897–907. https://doi.org/10.1104/pp.119.3.897 PMID: 10069828

46. Nomura T, Nakayama M, Reid JB, Takeuchi Y, Yokota T. Blockage of Brassinosteroid Biosynthesis and Sensitivity Causes Dwarfism in Garden Pea. Plant Physiol. 1997; 113:31–37. 113/1/31 [pii] PMID: 12223591

47. Koka CV, Cerny RE, Gardner RG, Noguchi T, Fujioka S, Takatsuto S, et al. A putative role for the tomato genes *DUMPY* and *CURL-3* in brassinosteroid biosynthesis and response. Plant Physiol. 2000; 122:85–98. https://doi.org/10.1104/PP.122.1.85 PMID: 10631252

48. Reid DE, Heckmann AB, Novák O, Kelly S, Stougaard J. *CYTOKININ OXIDASE/DEHYDROGENASE3* maintains cytokinin homeostasis during root and nodule development in *Lotus japonicus*. Plant Physiol. 2016; 170:1060–1074. https://doi.org/10.1104/pp.15.00650 PMID: 26644503

49. Wasilewska LD, Bralczyk J, Szczegielniak J. The role of gibberellin in regulation of dwarf plants development. Plant Sci. 1987; 53:11–19. https://doi.org/10.1016/0168-9452(87)90172-5

50. Dubois M, Van den Broeck L, Inzé D. The pivotal role of ethylene in plant growth. Trends in Plant Sci. 2018; 23(4):311–323. https://doi.org/10.1016/j.tplants.2018.01.003 PMID: 29428350

51. Vaseva II, Qudeimat E, Potuschak T, Du Y, Genschik P, Vandenbussche F, et al. The plant hormone ethylene restricts *Arabidopsis* growth via the epidermis. Proc Natl Acad Sci. 2018:201717649. https://doi.org/10.1073/pnas.1717649115 PMID: 29643073

52. Lee S, Choi SC, An G. Rice SVP-group MADS-box proteins, OsMADS22 and OsMADS55, are negative regulators of brassinosteroid responses. Plant J. 2008; 54:93–105. https://doi.org/10.1111/j.1365-313X.2008.03406.x PMID: 18182025

53. Wang L, Zeng XQ, Zhuang H, Shen YL, Chen H, Wang ZW, et al. Ectopic expression of *OsMADS1* caused dwarfism and spikelet alteration in rice. Plant Growth Regul. 2017; 81:433–442. https://doi.org/10.1007/s10725-016-0220-9

54. Kim TW, Michniewicz M, Bergmann DC, Wang ZY. Brassinosteroid regulates stomatal development by GSK3-mediated inhibition of a MAPK pathway. Nature. 2012; 482:419–422. https://doi.org/10.1038/nature10794 PMID: 22307275